Structural bases for understanding the stereoselectivity in ketone reductions with ADH from *Thermus thermophilus*: A quantitative model

Vittorio Pace [a], Álvaro Cortés Cabrera [b], Valerio Ferrario [c], José V. Sinisterra [a], Cynthia Ebert [c], Lucia Gardossi [c], Paolo Braiuca [c,d,*], Andrés R. Alcántara [a,**]

[a] *Departamento de Química Orgánica y Farmacéutica, Facultad de Farmacia, Universidad Complutense, Pza. Ramón y Cajal, s/n, 28040 Madrid, Spain*
[b] *Unidad de Bioinformática, Centro de Biología Molecular "Severo Ochoa" CSIC-UAM, C/Nicolás Cabrera 1, Campus UAM, 28049 Madrid, Spain*
[c] *Dipartimento di Scienze Chimiche e Farmaceutiche, Università degli Studi di Trieste, P.le Europa 1, 34127 Trieste, Italy*
[d] *SPRIN s.r.l., Viale XX Settembre 17, 34100 Trieste, Italy*

ARTICLE INFO

ABSTRACT

Automated structural analysis of alcohol dehydrogenase from *Thermus thermophilus* (*ADHTt*), a new carbonyl reductase recently described belonging to the SDR superfamily, allows to identify the aminoacidic residues responsible for the reductive catalytic activity, namely Ser-135, Tyr-148 and Lys-152. A series of acetophenone like compounds reduced with such enzyme was docked showing a distinct preference for binding to the active center. Favorable docking conformations calculated with two different protocols fall into two low-energy ensembles. These conformational ensembles are distinguished by the relative position of a given structure, presenting either the *si*- or *re*-face of the ketone to the nicotinamide mononucleotide (NMN) moiety reductant. For the ketones presented here, there is a correspondence between the major enantiomer obtained from the experimental data and the conformer found to have the most stable interaction energy with the receptor site in all cases. Furthermore, based on these two energy data sets we were able to build a reliable quantitative model ($R^2 = 0.98$; crossvalidation $q^2 = 0.78$) to predict the percentage of conversion from docking energy and the nature of the substrate with the following equation: conversion (%) = $30.80\,E_d - 72.84\sigma + 224.34$, where E_d is docking energy and σ is the Mulliken charge of the adjacent group of the ketone. The receptor site modeling, docking simulations, and enzyme–substrate geometry optimizations lead to a model for understanding the enantioselectivity of this NADH dependent carbonyl reductase.

© 2011 Elsevier B.V. All rights reserved.

1. Introduction

The asymmetric reduction of carbonyl compounds by microorganisms, a method outside the traditional arena of chemical synthesis, is now a well recognized as an invaluable tool for the preparation of chiral alcohols, which are important building blocks for a plethora of pharmaceuticals [1–4]. Thus, there is a constant demand for efficient biocatalysts for such fundamental transformations, and many new biocatalytic systems both in whole-cells and isolated enzymes forms have recently been developed [5–9]. Such isolated enzymes, namely oxidoreductases, belonging to one of three superfamilies, medium-chain alcohol dehydrogenases

(MDRs), short-chain dehydrogenase/reductases (SDRs), and aldo-keto reductases (AKRs). MDRs use zinc as catalyst [10], in contrast, the SDR which are non-metallo-oxidoreductases of about *ca.* 250-residue subunits, with a conserved Tyr-X-X-X-Lys motif and a Rossmann fold for NAD(P)H binding [11,12]. Finally, the AKRs, are monomeric proteins that bind nicotinamide cofactor without a Rossmann fold motif [13,14].

Recently, Raia and coworkers characterized and purified a novel highly enantioselective short-chain NAD(H)-dependent alcohol dehydrogenase from *Thermus thermophilus* [15], highlighting the exhibition of a Prelog specificity [16]. However, to the best of our knowledge, no molecular modeling studies supporting this enantioselectivity have been published yet.

Thus, as a part of our effort to develop an effective biocatalytic system to reduce a series of prochiral α-chloroketones, we considered appropriate to obtain mechanistic details about ketones reductions performed with *ADHTt*, starting from the experimental data reported by Raia, who showed the high performance of this ADH in reducing acetophenone like compounds. In order to achieve a robust and reproducible predictor system, we employed

* Corresponding author at: Dipartimento di Scienze Chimiche e Farmaceutiche, Università degli Studi di Trieste, P.le Europa 1, 34127 Trieste, Italy. Tel.: +39 040 558 3110; fax: +39 040 52572.
** Corresponding author. Tel.: +34 91 3941820; fax: +34 91 3941822.
E-mail addresses: braiuca@sprintechnologies.com (P. Braiuca), andresr@farm.ucm.es (A.R. Alcántara).

two different protocols, namely MOE based docking and molecular dynamics (MOE–DMD) [17] and Autodock4 [18] base docking with GROMACS [19] based molecular dynamics (ADGMX) to perform calculations on the crystal structure of *ADHTt* recently deposited in the Protein Data Bank [20] (PDB ID 2D1Y).

2. Experimental

2.1. MOE–DMD protocol

The molecular operating environment (MOE, version 2006.03) [17] program was used for all calculations. Molecular mechanics calculations utilize the Amber94 force field [21] and Marsilli–Gasteiger "Partial Equalization of Orbital Electronegativities" (PEOE) atomic charges [22].

2.2. Receptor sites in the ADHTt

The structure of *ADHTt* was downloaded from the Protein Data Bank [20]. Hydrogens were added to all atoms, taking care that the nicotinamide mononucleotide (NMN) moiety unit of the cofactor was reduced at carbon-4. As the 2D1Y crystal structure is composed by four identical enzyme units, only one of these monomer unit was used in the subsequent calculations. The enzyme geometry was then optimized in two steps. With the heavy atom positions fixed at their crystallographic positions, hydrogen atoms positions were geometry optimized. Then, the rest of the structure was also kept flexible during the optimization. Both sets of calculations were performed with the Amber94 force field [21]. Potential receptor sites within 2D1Y were identified using site algorithm within MOE, which utilized a geometry-based (as opposed to an energy based) technique, and which is based upon the alpha shape methodology [23,24]. Operating settings employed in this study were as follows: probe radius 1 = 1.4 Å (radius of a hypothetical, hydrogen-bonding atoms), probe radius 2 = 1.8 Å (radius of a hypothetical hydrophobic atom), isolated donor/acceptor = 3 Å (if a hydrophilic alpha sphere had no hydrophobic alpha sphere within the specified distance, then the former was discarded; this minimized sites likely to bind only water), connection distance = 2.5 Å (if individual clusters had two alpha spheres within this distance they were combined), minimum site size = 3 (minimum number of alpha spheres that comprised a suitable receptor site), radius = 2 Å (sites smaller than this size were eliminated). Solvent and salts were excluded in these simulations.

2.3. Docking simulations

Ketones reduced by Raia and coworkers were docked in a box that encompassed the two largest receptor sites found. The enzyme geometry was fixed, while the substrate geometry was flexible throughout these docking simulations. Water molecules in the vicinity of the receptor sites were deleted. To minimize the computational effort per run (and thus conduct more docking runs), a truncated receptor site model of 2D1Y was validated (residues included were those in a 7.5 Å radius of either of the largest receptor sites or the cofactor). Test docking simulations with acetophenone using the full enzyme did not lead to appreciably different results versus those obtained with the truncated receptor site model, so that the latter model was employed for other ketones. The Tabu search algorithm was employed for docking [25]. Tabu utilizes a list of previously visited conformations (in this case 100) to explore novel areas of docking space. 100 docking runs (each with a random starting geometry of substrate) were utilized. Each run entailed 1000 steps (maximum number of iterations in which the substrate was moved), and 100 attempts per

step (maximum number of substrate conformations explored per step).

2.4. Molecular dynamics

The lowest energy substrate/receptor site conformations for each ligand obtained from docking were submitted to molecular dynamics (NVT conditions, 300 K, 100 ps equilibration, 1 fs step size). Conformations for each compound from docking simulations were then geometry optimized using the Amber94 force field [21] and used to perform MD simulations. To maintain the structural integrity of a full enzyme model and to reduce the computational time, atoms lying out of a sphere of 10 Å radius centered on the substrate, were frozen during both the MD simulations and subsequent geometry optimization. To build the models, most favorable conformations were selected according to the following criteria: a favorable binding energy and the distance between NC4 atom of NADH and carbonyl of the ligand shorter than 4 Å to allow the hydride transfer, as postulated by Agarwal for other dehydrogenases [26].

2.5. ADGMX-protocol

In order to achieve reliable and reproducible molecular models of the selected ligands (Table 1), as a first step, before submitting docking and subsequent analysis, geometry optimization of the ground states were performed using the semi-empirical PM3 Hamiltonian (MOPAC 7.1) [27]. Finally, Gasteiger–Marsili atomic charge was chosen for the docking (Autodock default method) [22].
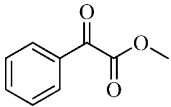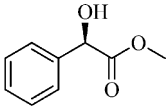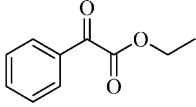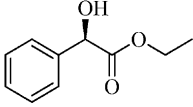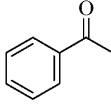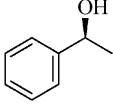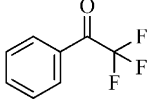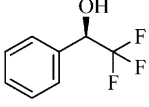
2.6. Receptor sites in the ADHTt

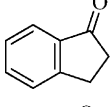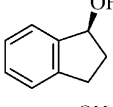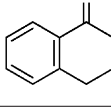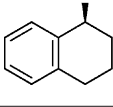As described before, the crystal structure of the alcohol dehydrogenase of *T. thermophilus* from Protein Data Bank [20] (PDB ID 2D1Y) was used as the protein model. From the original tetramer, the chain A and the bonded NADH cofactor were extracted discarding all water molecules attached to the protein. All the necessary hydrogen atoms were added using the default utility in the GROMACS software suite (version 4.0.3) [19] that assigns the different states of protonation according to the most favorable interactions between residues using geometrical parameters and known physicochemical properties. Subsequently, to avoid close contacts in the crystal structure, a 1000 steps conjugate gradient minimization of the system was performed and the resulting protein–NADH complex was used as starting point of docking and molecular dynamics studies. Energy minimization was performed with the GROMOS 96 43a1 force field [28], by setting 1 nm nonbonded cutoff and Particle-Mesh-Ewald summation [29] for electrostatic interactions. During minimization, root mean square deviation (RMSD) from the crystal structure of the protein was carefully observed to assure a very low model distortion (less than 0.02 nm for all ligand–protein complexes).

2.7. Docking and molecular dynamic parameters

All the docking studies were carried out by the program Autodock4 (version 4.0.3) [18] which allows a very fast energy evaluation using precomputed grids of affinity potentials for rigid docking. In order to explore the conformational space of the ligands, all torsional bonds in substrates were set free to perform flexible docking while the enzyme was kept rigid. Polar hydrogens and Gasteiger charges were assigned by the respective modules in Autodock Tools4 [18]. Despite the lack of ligand in the crystal enzyme used for this work, the grids were designed taking account of the reaction mechanism that involves the atoms in the proximity of the cofactor in order to be sure that the hydride transfer occurs.

Table 1
Asymmetric reduction of carbonyl compounds by *ADHTt* reported by Raia and coworkers [15].

Substrate	Product	Conversion (%)	ee (%)	Absolute configuration
(methyl phenylglyoxylate)	(methyl mandelate)	99	91	R
(ethyl phenylglyoxylate)	(ethyl mandelate)	90	95	R
(acetophenone)	(1-phenylethanol)	70	>99	S
(2,2,2-trifluoroacetophenone)	(2,2,2-trifluoro-1-phenylethanol)	100	93	R
(1-indanone)	(1-indanol)	40	>99	S
(1-tetralone)	(1-tetralol)	18	>99	S

For this reason all grids were centered near the cofactor and have a size of 60 × 60 × 60 grid points with a spacing of 0.375 Å between points, assuring coverage over the active site center and the surrounding area. All the grid maps used to represent the protein in the rigid docking were calculated by AutoGrid [18]. Docking of the compounds was carried out using the empirical free energy function and the Lamarckian genetic algorithm applying a standard protocol with an initial population of 150 randomly placed individuals, a maximum number of 2.4×10^7 energy evaluations, a mutation rate of 0.02, a crossover rate of 0.80, and an elitism value of 1.

The protocol was repeated fifty one times per compound. The results were clustered according to a RMSD criterion and classified taking the predicted energy of binding into account. Also by employing this calculation protocol, the most favorable conformations have been chosen according to the aforementioned Agarwal hypothesis [26] and the energetic criteria, as described in MOE–DMD protocol.

After selection of the most favorable poses, molecular dynamic simulations of the ligand–cofactor–enzyme systems were carried out using the GROMACS suite with the GROMOS 96 43a1 force field [28].

For each ligand, the most suitable conformations were tested once for each side (*pro-R* and *pro-S*). For some of the substrates, one of the two orientations is not among the poses generated by Autodock. In those cases a rotation of 180° of the most favorable side of the other "proenantiomer" performed to produce a *pro-R/pro-S* couple. All the topological parameters for the enzyme and NADH were created by GROMACS programs and the parameters of ligands were built by the Dundee PRODRG Beta Server [30]. Before performing a productive simulation, an energy minimization protocol consisting of 5000 steps of steepest descents (SD) minimization followed by a 5000 steps of Polak–Ribiere conjugate gradient (CG) [31] was carried out. After first minimization, the system was solvated in a SPC/E water box and the charges were neutralized with sodium ions. Before equilibrating the system, a new minimization was carried out following the same protocol. After-

wards, an equilibration simulation of 100 ps (NVT) with restraints in protein backbone and ligand position was performed. Finally a productive simulation of 300 ps at 300 K and 1 atm (NpT conditions) using the leapfrog algorithm with constraints in all bonds (LINCS algorithm) [32]. Particle-Mesh-Ewald summation [29] was applied dealing with long-range electrostatics and a 1.6 nm cut-off for Van der Waals interactions was used. The stability of the selected complexes was examined and snapshots of the MD trajectory were recorded every 1 ps. Also, the distance between NC4 of NADH and the ketone of the ligands was measured in order to predict the most probable conformation (*pro-R* or *pro-S*).

3. Results and discussion

The analysis of the ketones binding consists of three phases. First, receptor site in 2D1Y were identified. Second, substrates were docked into the receptor sites found in the first step; in this step, the substrate was flexible while the enzyme active site was fixed in its geometry. The third step entailed MD/energy minimization of receptor–substrate complexes for low energy docked conformations obtained from the second step.

3.1. NADH-binding site

The structure of the bound NADH, and interactions between this cofactor and amino acid residues are shown in Fig. 1. In the NMN, a nicotinamide ring adopts the *anti* conformation in a relationship between a carboxamide group and the ribose, and the ribose has the C2''-*endo* puckering conformation. Thus, the overall conformation of the bound NADH is very similar to that found in structure-solved enzymes belonging to the SDR family.

3.2. Substrate-binding model: docking studies

To study the docking of substrates into *ADHTt* active site, experimental data on the bioreduction of several acetophenone-like
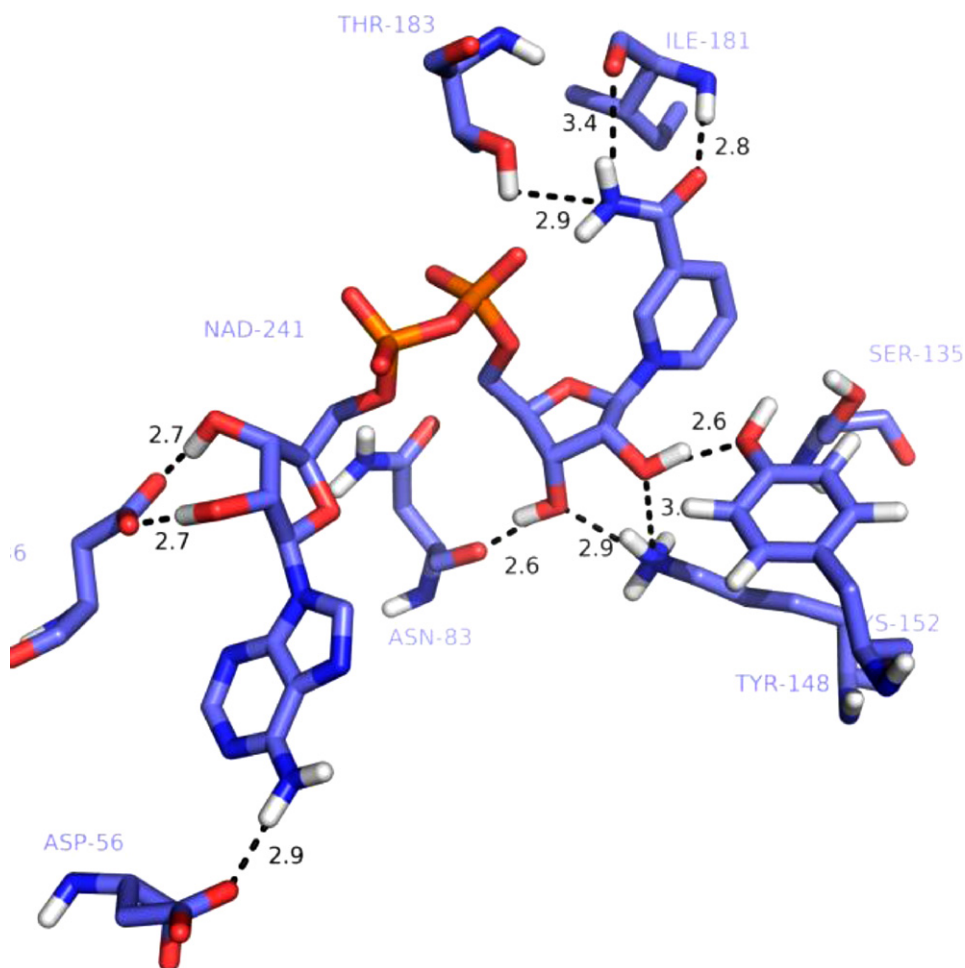
Fig. 1. Cofactor binding site of *Thermus thermophilus* ADH.

compounds were taken from the work of Raia and coworkers [15] which are summarized in Table 1.

Several interesting features were identified from the docking simulations. First, docking of the ketones is energetically preferred in the catalytic portion of the combined catalytic/hydrophilic receptor site, shown in green in Fig. 2, which is close to the NADH binding area (Fig. 2, blue).

According to the proposed catalytic mechanism of the enzymes belonging to the SDR family [33] three catalytic residues (Tyr, Ser and Lys) are essential for the catalytic reaction. The carbonyl oxygen atom of a substrate forms hydrogen bonds with Ser-135, while maintaining very close to Tyr-148. It may be assumed that the carbonyl oxygen of the substrate is protonated from the Tyr residue, followed by the attacking of the hydride from the C4 atom of NADH to the carbonyl carbon atom (presenting a high electrophilicity due to the H bond) as shown in Scheme 1. In addition, Asn-145, which is close to the Tyr-148 residue while being in contact with the solvent may act as a transport system to transfer new protons from the bulk solvent to the active center [33] allowing the reprotonation of the Tyr-148.

In other SDR families, the Lys residue forms a direct hydrogen bond with the Tyr residue [33] however, in this *ADHTt*, Lys-152

makes a hydrogen bond with the O2″ atom of NMN (Fig. 1) and the O2″ atom donates hydrogen atoms to the OH atom of Tyr-148, as shown in Fig. 3.

Acetophenone was selected as the reference compound to describe the binding mode and interactions with the protein and cofactor. First, as can be seen in Fig. 3, Ser-135, stabilizes the substrate with a hydrogen bond according to geometrical parameters (2.6 Å between heavy atoms and an angle of 172.1°, very close to 180°), while the phenyl ring is embedded in a hydrophobic cavity next to the catalytic center composed mainly for Val-136, Gly-179, Ala-180, Trp-195, Leu-198 and Met-236. These two interactions allow the ketone to be placed at a distance of 3.6 Å (calculated from the NC4 atom and the carbonylic carbon), closed enough for the hydride transfer. For the rest of docked compounds, similar behavior is observed due to a high structural similarity. These compounds have in common an aromatic ring vicinal to a ketone, and these groups are the essential features of the binding mode exposed before. The docked conformations ensembles are distinguished by the positions of the substituents, presenting either the *si* or *re*-face of the ketone to the nicotinamide reductant. Fig. 4 shows an overlay of the lowest energy conformations obtained by docking the Raia reduced ketones to the truncated catalytic site of 2D1Y.
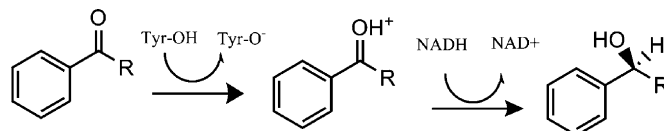
Scheme 1. Scheme of bioreduction catalyzed by ADH of *Thermus thermophilus*.
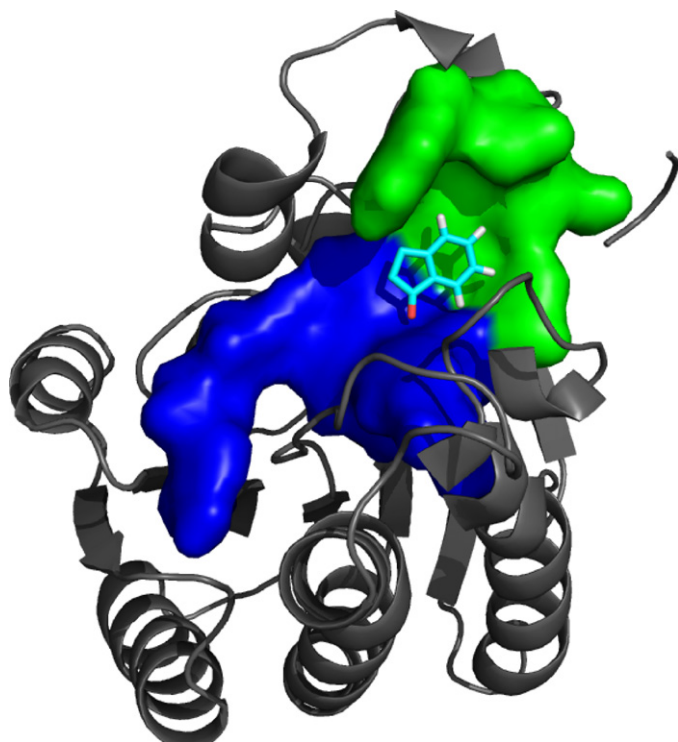
Fig. 2. NADH binding area (blue) and hydrophobic substrate-binding area (green) in *ADHTt*, exemplified for 1-indanone docking. (For interpretation of the references to color in this figure legend, the reader is referred to the web version of the article.)

It is important to stress that ketones bearing a bicyclic system, thus presenting more rigid conformations, namely 1-indanone and α-tetralone, have been reduced with lower rate of conversion. This observation suggests that flexibility between ketone and aromatic ring is possibly necessary for achieving high performance reduction.

In Table 2, docking energies obtained by using the two calculation protocols MOE–DMD and ADGMX are shown. As can be seen there is a perfect agreement between the two different algorithms and energy evaluation functions, giving enough confidence for a quantitative model.

With the aim of achieving a quantitative model, the Autodock binding energies were correlated with the percentage of conversion at 5 h (excluding MBF), achieving a not completely satisfactory coefficient ($R^2 = 0.76$) and pointing out that specific compound related features should be taken into account. Bearing in mind this fact, the electronic properties of substituents have been considered in the regression employing the Mulliken charges of the neighbor groups from density functional theory (DFT) calculations. DFT charges were obtained using Becke's three-parameter Lee–Yang–Par (B3LYP) functional and 6-31G++(d,p) basis by means of the Massively Parallel Quantum Chemistry (MPQC) program [34]. This extra variable represent the electronic effect over the carbonyl carbon atom that could influence the nucleophilic attack of the hydride from the NADH cofactor which has been found a key factor in previous works on ketone reductions [35].

Multivariable linear regression test was carried out on the new two-variables data set, using the software GNU/PSPP [36]. The results represent a significant improvement in fitting ($R^2 = 0.977$)
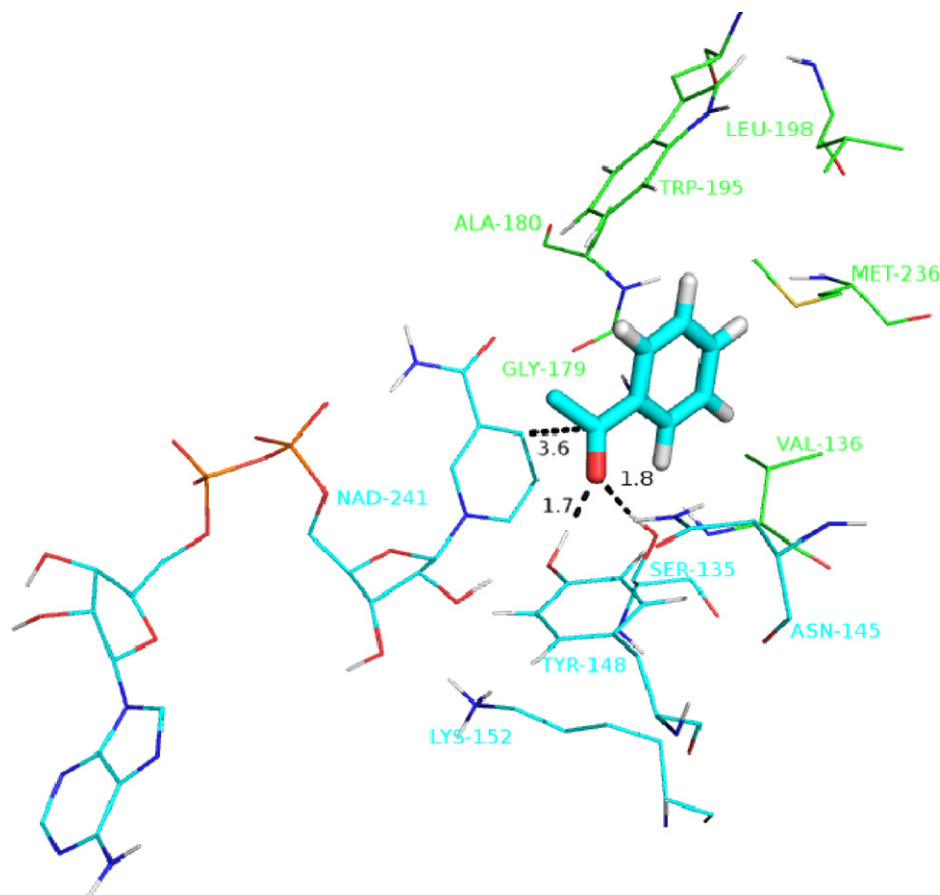

Fig. 3. The lowest energy docking conformations of acetophenone and NADH in the enzyme active site. The hydride of the C-4 atom of the nicotinamide ring attacks at the carbonyl carbon of acetophenone from the *re*-face, leading to the (*S*) enantiomer of 1-phenylethanol. In green, residues of the hydrophobic pocket near the catalytic center (shown in blue). (For interpretation of the references to color in this figure legend, the reader is referred to the web version of the article.)

Table 2
Comparative study of binding energy calculated on docked conformations.

Compound	E_{BAD}[a] (kcal/mol)	E_{BMOE}[b] (kcal/mol)	Product[c] (experimental)	Product[d] (predicted)	σ[e]
Methyl benzoylformate (MBF)	−4.95	−4.87	R	R	−
Ethyl benzoylformate (EBF)	−5.14	−5.20	R	R	−0.390
Acetophenone	−4.99	−5.04	S	S	0.001
2,2,2-Trifluoroacetophenone	−4.77	−4.86	R	R	−0.210
1-Indanone	−5.23	−5.11	S	S	0.320
α-Tetralone	−6.05	−6.15	S	S	0.250

[a] Autodock binding energy.
[b] MOE binding energy.
[c] Experimental configuration of the product.
[d] Predicted configuration of the product.
[e] Mulliken charges of ketone adjacent groups.

with respect to the energy-only based model. This new model is represented by the following equation:

$$Conversion(\%) = 30.80E_d - 72.84\sigma + 224.34$$

shown in Fig. 5, where E_d is the docking energy and σ is the electronic term. This model also was able to reproduce the conversion percentage of the compounds with a mean error of 4.11%.

To validate the model, "leave-one-out" (LOO) cross-validation was performed, using q^2 as indicator of the predictive performance according to the following formula:

$$q^2 = 1 - \frac{\sum (y_i - \hat{y}_i)^2}{\sum (y_i - \bar{y})^2}$$

where y_i is the actual conversion percentage, $\bar{y}$ is the average actual conversion percentage, and $\hat{y}_i$ is the predicted conversion of compound i, obtained from each new regression. The resulting cross-validation coefficient, $q^2 = 0.778$, give an acceptable confidence in the predictive capacity of the model.

3.3. Molecular dynamics

All trajectories appeared to be equilibrated after 70 ps, based on the energy trend of the system and a stable C-alpha RMSD of the protein close to 1.5 Å which is the resolution of crystal structure. In all cases, the analysis of trajectories from both protocols confirms qualitatively the docking results and the binding mode; simulations performed with less favorable or rotated conformers follow two trends: displacement from the active center (Fig. 6) or turn into a nonproductive conformation (Fig. 7). The first behavior has been observed in the cases of 2,2,2 trifluoroacetophenone *pro-S* and EBF *pro-S*. Otherwise, a non productive conformation has been noticed
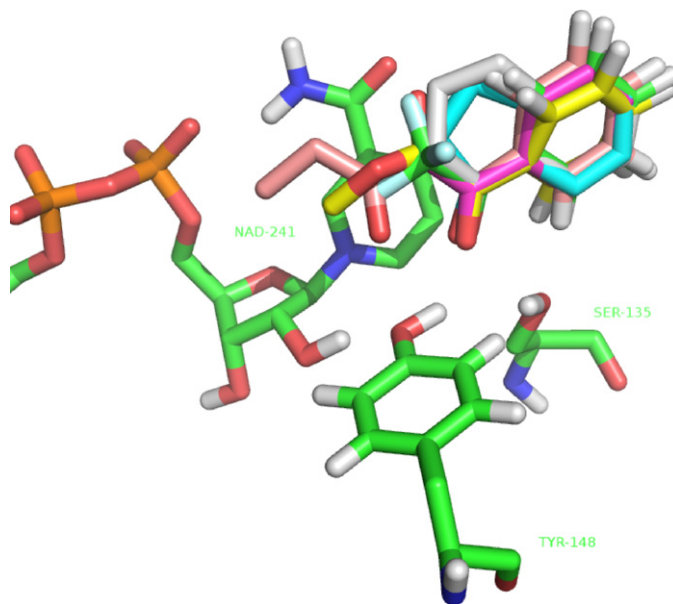

Fig. 4. Overlay of lowest energy docked conformations of EBF (gray), 1-indanone (orange), α-tetralone (pink), acetophenone (yellow), 2,2,2-trifluoroacetophenone (light blue), MBF (dark blue). (For interpretation of the references to color in this figure legend, the reader is referred to the web version of the article.)

with acetophenone *pro-R*, 1-indanone *pro-R*, α-tetralone *pro-R* and MBF *pro-S*.

This behavior is shown in the measure of the distance between the C4 and the ketone carbon (Figs. 8 and 9). In the predicted confor-
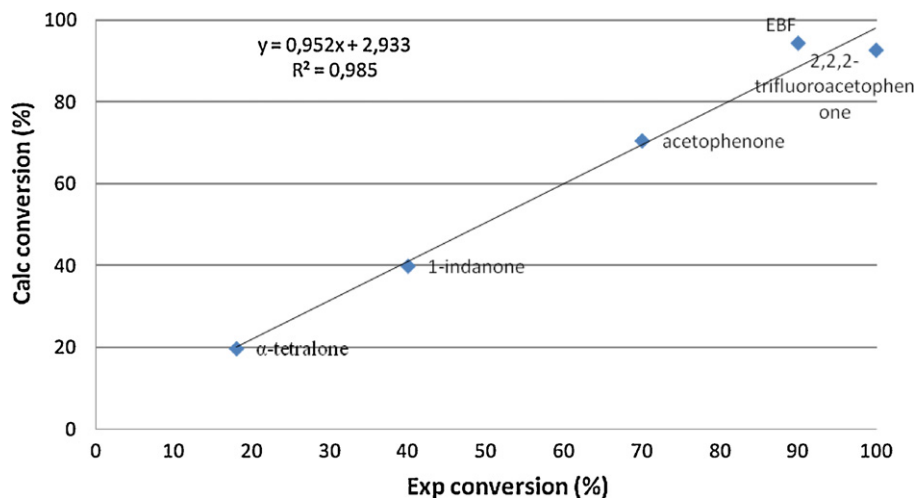

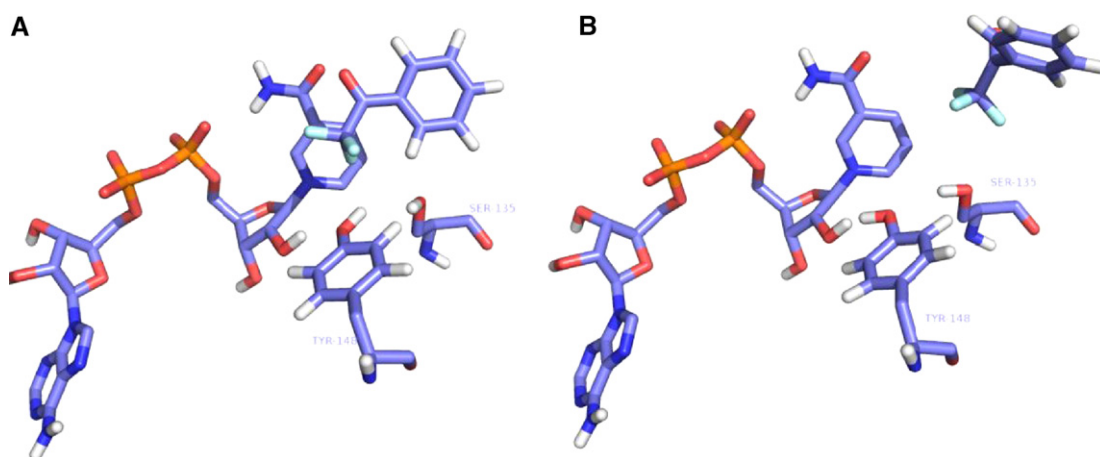**Fig. 5.** Fitting of calculated versus experimental conversion.

Fig. 6. Conformational change observed for 2,2,2-trifluoroacetophenone *pro-S*: (A) initial docked conformation and (B) conformation after 300 ps.
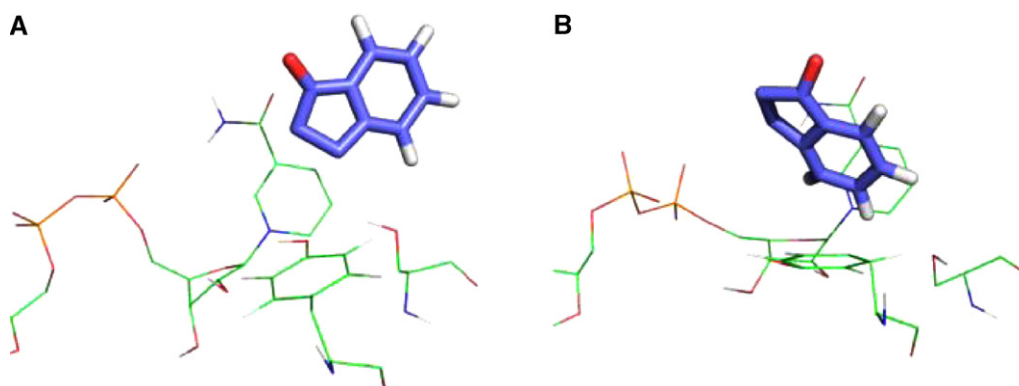

Fig. 7. Conformational change observed for 1-indanone *pro-R*: (A) initial docked conformation and (B) conformation after 300 ps.
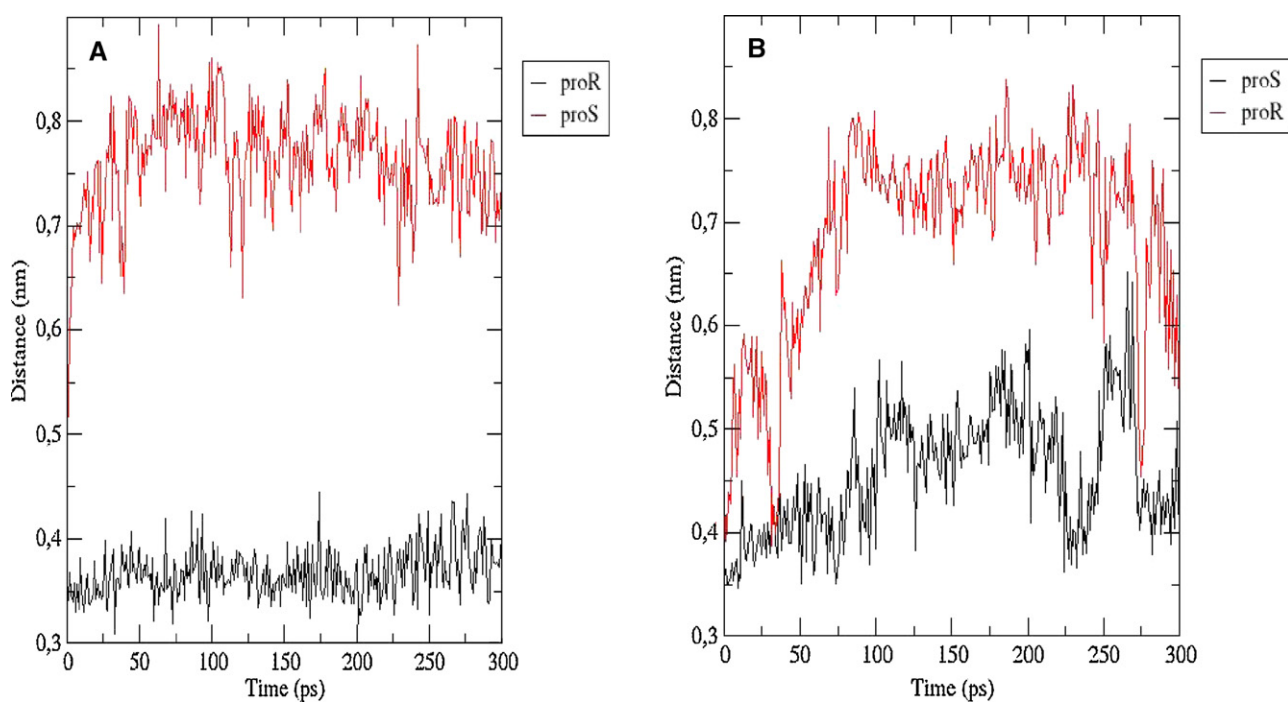

Fig. 8. Variation of the distance between the C4 atom of NADH and the carbonylic carbon during the simulation for EBF (A) and 2,2,2-trifluoroacetophenone (B).
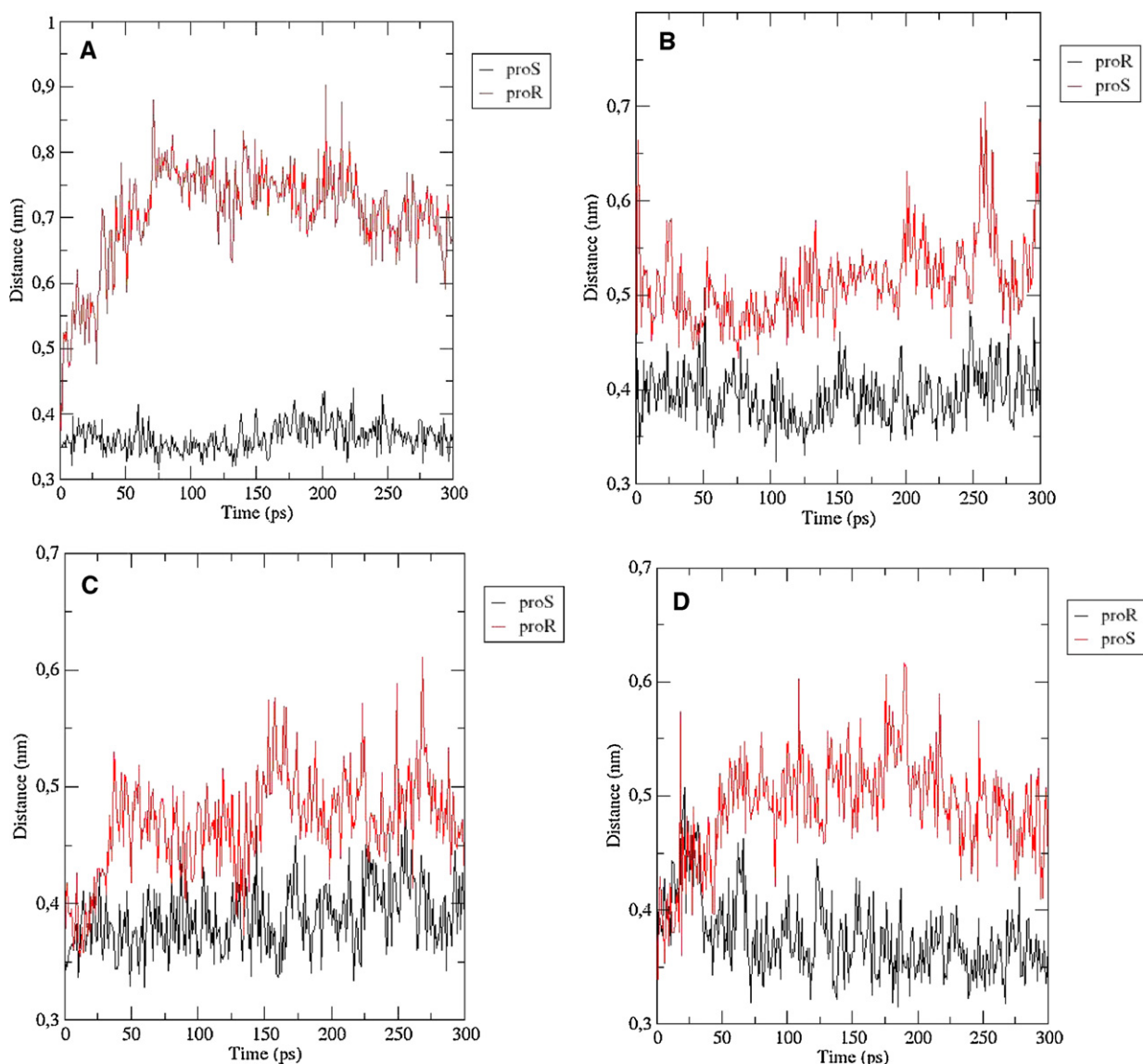
Fig. 9. Variation of the distance between the C4 atom of NADH and the carbonylic carbon during the simulation: (A) 1-indanone, (B) acetophenone, (C) α-tetralone and (D) MBF.

mation this distance hardly becomes greater than 4 Å meanwhile in the alternative conformation is too far from NADH, so no reduction can be expected according to Agarwal theoretical study on ADH [26].

The reason of the change in the alternative conformation is the lack of the hydrogen bond with Ser-135 residue, a key interaction to maintain a productive conformation, positioning the ketone group in front of the cofactor. It is worth noting also that additional hydrogen bonds can exist in some compounds. In the case of EBF an extra hydrogen bond between the oxygen of the second ketone and the O3″ hydroxyl group of the NADH due to the syn disposition forced by the ethyl chain is found in the docked conformation and in the trajectories. MOE based MD trajectories show the same trends (results not shown).

4. Conclusions

On the basis of the docking and molecular dynamics simulations, several residues essential for the catalytic mechanism in *ADHTt* were identified. According to Filling et al. [33], we postulate a Tyr-Lys-Ser-Asn catalytic tetrad. In our model, Ser-135 plays

an important role stabilizing the substrate with a hydrogen bond anchoring the ketone near the NADH, Tyr-148 provides the hydrogen atom in the reductive reaction direction, meanwhile positively charged Lys-152 stabilizes the deprotonated residue and Asn-145 transfers new protons from the bulk solvent to the active center as a "proton relay system". In addition to the catalytic residues, and as uniqueness of our model, a group of hydrophobic residues have been found, namely Val-136, Gly-179, Ala-180, Leu-198, Trp-195 and Met-236, that stabilize the aromatic ring of the substrate and give the resulting product stereochemistry.

Furthermore, we have shown a detailed stereochemical mechanistic pathway of the bioreductions of different experimental reduced ketones with this ADH based on docking and molecular dynamics studies using two different scoring functions and force fields.

The fact that the two protocols employed estimate the binding energy values in, practically, the same manner guarantees a high confidence of the proposed method, thus representing a good starting point for the evaluation of other potential substrates to be reduced with this ADH. In fact, we propose a quantitative model that allows predicting, with a minimum error, the conversion rate

of the compounds by considering in the approximation the docking energies and a parameter concerning the electronic properties of the ketone.

The receptor site model summarized in Figs. 2 and 3 not only rationalizes the observed stereospecificity of *ADHTt* reductions of acetophenone like compounds, but also provides a starting point for identifying point mutations to active site residues that can enhance selectivity and activity, as well as broaden the scope of possible substrates. In fact, we are undergoing a parallel *in vitro* and *in silico* study of the bioreduction of new α-haloketones recently prepared in our group [37–39] not possessing an aromatic ring conjugated with the carbonyl function, catalysed by *ADHTt* and, preliminary results are in accordance with the proposed model.

Acknowledgments

References

[1] K. Faber, Biotransformations in Organic Chemistry. A Textbook, 5th ed., Springer-Verlag, Berlin, Heidelberg, 2004.
[2] J. Moore, D. Pollard, B. Kosjek, P. Devine, Acc. Chem. Res. 40 (2007) 1412–1419.
[3] S. Wildeman, T. Sonke, H. Schoemaker, O. May, Acc. Chem. Res. 40 (2007) 1260–1266.
[4] T. Matsuda, R. Yamanaka, K. Nakamura, Tetrahedron-Asymmetr. 20 (2009) 513–557.
[5] K. Edegger, W. Stampfer, B. Seisser, K. Faber, S. Mayer, R. Oehrlein, A. Hafner, W. Kroutil, Eur. J. Org. Chem. 2006 (2006) 1904–1909.
[6] T. Ema, H. Yagasaki, N. Okita, M. Takeda, T. Sakai, Tetrahedron 62 (2006) 6143–6149.
[7] I. Kaluzna, T. Matsuda, A. Sewell, J. Stewart, J. Am. Chem. Soc. 126 (2004) 12827–12832.
[8] T. Poessl, B. Kosjek, U. Ellmer, C. Gruber, K. Edegger, K. Faber, P. Hildebrandt, U. Bornscheuer, W. Kroutil, Adv. Synth. Catal. 347 (2005) 1827–1834.
[9] P. Soni, G. Kaur, A. Chakraborti, U. Banerjee, Tetrahedron-Asymmetr. 16 (2005) 2425–2428.
[10] H. Jörnvall, M. Persson, J. Jeffery, Proc. Natl. Acad. Sci. U.S.A. 78 (1981) 4226.
[11] H. Joernvall, B. Persson, M. Krook, S. Atrian, R. Gonzalez-Duarte, J. Jeffery, D. Ghosh, Biochemistry-US 34 (1995) 6003–6013.
[12] U. Oppermann, C. Filling, M. Hult, N. Shafqat, X. Wu, M. Lindh, J. Shafqat, E. Nordling, Y. Kallberg, B. Persson, Chem.-Biol. Interact. 143 (2003) 247–253.
[13] K. Bohren, B. Bullock, B. Wermuth, K. Gabbay, J. Biol. Chem. 264 (1989) 9547.
[14] J. Jez, M. Bennett, B. Schlegel, M. Lewis, T. Penning, Biochem. J. 326 (1997) 625.
[15] A. Pennacchio, B. Pucci, F. Secundo, F. La Cara, M. Rossi, C. Raia, Appl. Environ. Microbiol. 74 (2008) 3949.
[16] V. Prelog, Pure Appl. Chem. 9 (1964) 119–130.
[17] I. Chemical Computing Group, MOE-2006.03, Montreal, Canada, 2006.
[18] G. Morris, R. Huey, W. Lindstrom, M. Sanner, R. Belew, D. Goodsell, A. Olson, J. Comput. Chem. 30 (2009) 2785–2791.
[19] B. Hess, C. Kutzner, D. van der Spoel, E. Lindahl, J. Chem. Theory Comput. 4 (2008) 435–447.
[20] H. Berman, T. Battistuz, T. Bhat, W. Bluhm, P. Bourne, K. Burkhardt, Z. Feng, G. Gilliland, L. Iype, S. Jain, Acta Crystallogr. D 58 (2002) 899–907.
[21] W. Cornell, P. Cieplak, C. Bayly, I. Gould, K. Merz, D. Ferguson, D. Spellmeyer, T. Fox, J. Caldwell, P. Kollman, J. Am. Chem. Soc. 117 (1995) 5179–5197.
[22] J. Gasteiger, M. Marsili, Tetrahedron 36 (1980) 3219–3228.
[23] J. Liang, H. Edelsbrunner, P. Fu, P. Sudhakar, S. Subramaniam, Proteins 33 (1998) 1–17.
[24] J. Liang, H. Edelsbrunner, P. Fu, P.V. Sudhakar, S. Subramaniam, Proteins 33 (1998) 18–29.
[25] C. Baxter, C. Murray, D. Clark, D. Westhead, M. Eldridge, Proteins 33 (1998) 367–382.
[26] P. Agarwal, S. Webb, S. Hammes-Schiffer, J. Am. Chem. Soc. 122 (2000) 4803–4812.
[27] M. Otyepka, V. Krystof, L. Havlic ek, V. Siglerova, M. Strnad, J. Koca, J. Med. Chem. 43 (2000) 2506–2513.
[28] L. Schuler, X. Daura, W. Van Gunsteren, J. Comput. Chem. 22 (2001) 1205–1218.
[29] T. Darden, D. York, L. Pedersen, J. Chem. Phys. 98 (1993) 10089–10092.
[30] A. Schuttelkopf, D. van Aalten, Acta Crystallogr. D 60 (2004) 1355–1363.
[31] L. Grippo, S. Lucidi, Math. Program. 78 (1997) 375–391.
[32] B. Hess, H. Bekker, H. Berendsen, J. Fraaije, J. Comput. Chem. 18 (1997) 1463–1472.
[33] C. Filling, K. Berndt, J. Benach, S. Knapp, T. Prozorovski, E. Nordling, R. Ladenstein, H. Jörnvall, U. Oppermann, J. Biol. Chem. 277 (2002) 25677.
[34] C. Janssen, I. Nielsen, M. Leininger, E. Valeev, E. Seidl, Sandia National Laboratories, 2004.
[35] B. Ganguly, J. Chandrasekhar, F. Khan, G. Mehta, J. Org. Chem. 58 (1993) 1734–1739.
[36] GNU/PSPP, Free Software Foundation, Boston, USA, 2007.
[37] V. Pace, F. Martínez, M. Fernández, J.V. Sinisterra, A.R. Alcántara, Adv. Synth. Catal. 351 (2009) 3199–3206.
[38] V. Pace, G. Verniest, J.V. Sinisterra, A.R. Alcántara, N. De Kimpe, J. Org. Chem. 75 (2010) 5760–5763.
[39] V. Pace, A. Cortés-Cabrera, M. Fernández, J.V. Sinisterra, A.R. Alcántara, Synthesis 20 (2010) 3545–3555.